Characterization and Optimization of Two-Body Abrasive Wear in Tropical Hardwoods: A Materials Engineering Approach

Aubin Takoudjou talla
takoudjouaubin@gmail.com

University of Dschang https://orcid.org/0000-0003-3539-9800

Rene Ngouffo Koukougnang
ngouffo2002@yahoo.fr

University of Buea

Ulrich Azeufack Tonfack
University of Buea https://orcid.org/0009-0005-0548-0159

Jeanne Sandrine Mabekou Takam
University of Dschang

Pierre Kisito Talla
University of Dschang https://orcid.org/0000-0003-2987-9322

Research Article

Keywords: Wear coefficient, Tropical hardwoods, Sliding abrasion, Sliding speed, Tribological behavior, Surface degradation

Posted Date: July 24th, 2025

DOI: https://doi.org/10.21203/rs.3.rs-7182910/v1

Additional Declarations: The authors declare no competing interests.

Abstract

This study investigates the abrasive wear behavior of three tropical hardwood species *Tieghemella heckelii* (makore), *Khaya anthotheca* (mahogany), and *Pericopsis elata* (assamela) under varying loads and sliding speeds. Two-body abrasion tests were performed perpendicular to the fiber orientation using a Taber abrasimeter equipped with P120 aluminum oxide wheels. Tests were conducted under dry conditions at rotational speeds ranging from 20 to 70 rpm and loads of 250 g, 500 g, and 750 g. The wear coefficient (k) was calculated from the linear region of the wear volume versus sliding distance curve, representing the steady-state regime where the wear mechanism is stabilized. All species displayed a linear wear-volume relationship, confirming the relevance of Archard's law. Among the tested species, assamela exhibited the lowest wear rates, while makore showed the highest. Interestingly, the wear coefficient decreased with increasing load, particularly between 250 g and 500 g, suggesting improved fiber compaction and reduced interfacial fragmentation under higher pressures. Sliding speed effects were nonlinear and species-dependent. Makore performed best at higher speeds and heavier loads, whereas mahogany displayed dual behavior optimized either under high-speed/low-load or low-speed/high-load conditions. Assamela showed more stable performance, with minimal wear occurring at intermediate speeds (50–60 rpm). Overall, the results highlight the critical interplay between wood anatomy, normal load, and sliding velocity in governing wear behavior. Identifying species specific operating regimes offers valuable insights for improving the durability of wood in applications involving mechanical contact and frictional stress.

1. INTRODUCTION

Wood is a sustainable and widely used material in both structural and decorative engineering applications due to its favorable mechanical properties, renewability, and broad availability. However, in contexts involving frictional contact or surface abrasion such as flooring, furniture, or tool handles its surface integrity may deteriorate over time. Therefore, understanding the wear resistance of wood under various mechanical and kinematic conditions is critical for ensuring material reliability and proper selection in engineering design.

Recent tribological studies have shown that wear in wood is not only species-dependent but also strongly influenced by operational parameters such as normal load and sliding speed. For instance, Wu et al. (2025) demonstrated that densified wood subjected to different loads and speeds exhibits increasing wear volume and friction coefficients, with sliding speed occasionally mitigating wear effects by altering the dominant abrasion mechanisms. Similarly, Snow et al. (2022) confirmed that thermo-mechanical densification significantly enhances abrasion resistance in several U.S. hardwood species, underscoring the role of internal structure in surface durability. Nasir and Cool (2018) also highlighted the influence of fiber orientation and mechanical anisotropy, showing that the direction of loading relative to grain structure modulates wear rates, thereby emphasizing the need to account for both mechanical and structural variables.

In engineered wood systems, surface wear and machining performance are further affected by the interaction between tool geometry and processing conditions. Torkghashghaei et al. (2022) demonstrated that optimizing the micro-geometry of carbide-tipped cutting tools using PVD coatings results in measurable reductions in wear rates during sawmill operations, underscoring the importance of tool–material contact dynamics. Likewise, Gendvilas et al. (2024) investigated resistance drilling in hardwoods and revealed that variations in feed rate and spindle rotation significantly influence drilling precision and indirectly reflect the wood's response under frictional stress. In a similar vein, Ghadiri et al. (2021) showed that increased cutting speeds during milling of laminated wood composites can induce thermal softening, altering the wear mechanism from abrasive to adhesive and thereby modifying wear behavior.

Recent studies on the thermo-hydro-mechanical (THM) densification of tropical hardwoods have further highlighted the potential for improving wear resistance through structural modification. In Costa Rica, Tenorio and Moya (2020) reported that THM densification of species such as *Alnus acuminata*, *Vochysia ferruginea*, and *V. guatemalensis* enhances both compressive strength and abrasion durability, confirming their suitability for flooring applications. Similarly, Zhou et al. (2019) demonstrated that surface densification of poplar (*Populus tomentosa*) improves the density profile and hardness, both of which are directly linked to abrasion resistance. At the microstructural level, Leiter et al. (2022) investigated triboelectric surface activation and found that brushing, thermal, and mechanical treatments alter surface energy and sliding behavior, affecting friction and wear interactions.

Despite these advances, relatively few studies have examined the wear behavior of West African tropical hardwoods under combined variations of normal load and sliding speed. In particular, species such as *Thieghemella heckelii* (makore), *Khaya anthotheca* (African mahogany), and *Pericopsis elata* (assamela) are highly valued in both local and international markets, yet their tribological response to mechanical abrasion remains poorly documented.

This study aims to fill that knowledge gap by characterizing the influence of load and sliding speed on the wear resistance of these three tropical hardwood species under two-body abrasion conditions. By identifying species-specific wear behaviors and optimal performance regimes, the results will support more informed material selection for high friction applications and contribute to the broader valorization of forest resources in Central Africa.

2. MATERIALS AND METHODS

2.1. Wood Species Selection and Specimen Preparation

In this study, three tropical hardwood species Makore (*Tieghemella heckelii*), Mahogany (*Khaya anthotheca*), and Assamela (*Pericopsis elata*) were selected due to their frequent use in mechanical wear applications such as flooring and industrial components. Test specimens were circular, with a diameter of 112 mm and a thickness of 7 mm, and were machined in the longitudinal direction of the wood. This orientation allowed the abrasion process to occur perpendicularly to the wood grain (Fig. 1c), simulating conditions where surface wear is most critical. The basic characteristics of the studied species are recorded in Table 1.

Table 1
Physical and mechanical properties of species

Species	MOR in static bending (MPA)		MOE in static bending (MPA)		Density (Kg/m^3)	
	Value	Humidity	Value	Humidity	Value	Humidity
MAKORE	46 ± 4	14	9711 ± 3461	14	654 ± 30	14
ASSAMELA	67 ± 7	14	9647 ± 1849	14	669 ± 67	14
MAHOGANY	46 ± 4	14	7911 ± 493	14	711 ± 26	14

2.2. Experimental Setup and Test Conditions

Wear tests were conducted using a Taber abrasimeter (Model DH-TA-01) (Fig. 1a), equipped with two aluminium oxide abrasive wheels (P120 grit). These wheels apply a constant vertical load on the rotating wood specimens to simulate surface friction under abrasive conditions. The tests were performed in dry, non-lubricated conditions, using three normal loads: 250 g, 500 g, and 750 g.

The rotational speed of the specimen holder was varied from 20 to 70 rpm in 10 rpm increments, producing a sliding distance of approximately 4 meters per test. Each condition was replicated for the three wood species.

2.3. Debris Management and Measurement of Mass Loss

To ensure consistent abrasive contact, a suction nozzle was installed directly above the wear track to eliminate wood particles generated during testing. After each test, specimens were carefully brushed to remove residual particles and weighed using a MY WEIGH electronic balance with an accuracy of ± 0.01 g (Fig. 1b). The mass loss (Δm) due to wear was then calculated by subtracting the final mass from the initial mass.

2.4 Calculation of worn volume

The volume of material removed (V) was calculated using the mass loss and the density of each species, as follows:

$$V = \Delta m / \rho$$

1

where: Δm is the mass loss (g) and ρ is the density of the wood species (g/cm³),

2.5 CALCULATION OF THE WEAR COEFFICIENT

To evaluate the wear behavior under varying operational conditions, the wear coefficient (k) was determined based on Archard's wear law:

$$k = V / F.D$$

2

where: V is the wear volume (mm^3), F is the applied normal load (N), and d is the sliding distance (m).

However, to improve accuracy and account for the transitional and steady-state wear behavior, the wear coefficient was computed from the slope of the linear portion of the wear volume versus sliding distance curve, corresponding to the steady-state regime. In this regime, the wear mechanism is stabilized, and the volume loss progresses linearly with distance.

The identification of the steady-state region was done by plotting the cumulative wear volume over increasing sliding distance, and selecting the portion where a linear trend with minimal fluctuation was observed.

All tests were performed at the Laboratory of Physical Systems Modelling (U2MSP), University of Dschang, under ambient environmental conditions: temperature of 24 ± 2°C and relative humidity of 65 ± 5%.

3. RESULTS AND DISCUSSION

3.1 BEHAVIOR DEPENDING ON THE WEAR DISTANCE TRAVELED

The results obtained for the evolution of wear volume as a function of rolling distance (Fig. 2) show two clearly distinct wear regimes: an initial runningin period, lasting approximately 0.138 m, followed by a steadystate wear region. This behavior aligns closely with classical tribological observations across a range of materials, including metals, polymers, and hard coatings (Okokpujie et al., 2024).

During the runningin phase, surface asperities are progressively removed or deformed, leading to a rapid increase in wear volume followed by stabilization (Sakhamuri, 2023). Similar phenomena have been reported for steels, where the wear rate and friction coefficient increase sharply during the runningin, and then plateau once the surface has adapted (Zambrano et al, 2024).

In our wood abrasion tests, the transition at 0.138 m suggests that a critical surface conditioning occurs smoothing peaks and densifying the contact interface after which wear volume grows linearly with rolling distance. This is consistent with the Archard wear model, where the steady-state wear coefficient becomes constant under stable contact conditions.

Importantly, this two-stage behavior was consistent across all tested speeds (20 rpm to 70 rpm), indicating that while sliding speed and load likely affect the magnitude of wear, they do not alter the fundamental wear mechanism. This mirrors findings in polymer-metal systems, where regardless of speed, materials exhibit this bifurcation of wear regimes (Abdelbary, 2021).

3.2 WEAR IN STATIONARY STATE AND WEAR COEFFICIENT

To evaluate the wear behavior of the three wood species under different loading and speed conditions, the wear coefficient was calculated using the slope of the linear portion of the wear volume versus sliding distance curve (Fig. 2), corresponding to the steady-state wear region. In that regime, the wear rate becomes constant, and the wear mechanism stabilizes, making the calculation of the wear coefficient (k) physically meaningful because the variation of the wear volume as a function of the sliding distance at different load reveals that all three wood species generally follow the linear trend predicted by Archard's wear law across all test sliding speed. This suggests that the increase in wear is, to a first approximation, directly proportional to the sliding distance (Zhai et al., 2021).

3.3 INFLUENCE OF LOAD ON WEAR COEFFICIENT

As shown in Fig. 3, the experimental results reveal a progressive decrease in the wear coefficient as the applied load increases from 250 g to 750 g, across all tested sliding speeds. This trend diverges from conventional tribological models, where increasing load typically leads to greater material loss due to intensified contact stress. In our study, a steep negative slope is observed between 250 g and 500 g, indicating a significant reduction in wear in this initial range. Beyond 500 g, although the slope remains negative, the decline is more moderate, suggesting a stabilization of the tribological behavior under high loading conditions.

This phenomenon can be explained by the progressive compaction of the wood's cellular structure under increasing loads. Such compaction enhances internal fiber cohesion, reducing breakage or fiber pull-out during abrasive interaction. Additionally, higher loads promote an increase in the real contact area, which in turn lowers the specific pressure exerted by the abrasive grains and limits their penetration depth into the material. These combined effects reduce the aggressiveness of the abrasive contact, especially for dense species such as makoré and assamela, which exhibit better resistance to localized plastic deformation.

Moreover, under high loading, an auto-adjusting or self-polishing mechanism may emerge, wherein micro-asperities are rapidly sheared off, producing a more uniform and smoother surface that is less susceptible to mechanical degradation. Therefore, our findings suggest the existence of a tribological stabilization zone beyond 500 g, where wear mechanisms become less sensitive to additional load. Although atypical, this behavior aligns with the unique microstructural properties of the tested tropical hardwoods, including high density, low porosity, and the perpendicular orientation of fibers relative to the sliding direction

3.4 INFLUENCE OF WEAR RATE ON WEAR COEFFICIENT

The variation of the wear coefficient as a function of rotational speed, for each applied load, revealed a non-monotonic trend across the three investigated wood species (Fig. 4). In contrast to the linear response typically expected from Archard's law under stable contact conditions, the wear coefficient exhibited both minima and maxima at specific speed intervals. This pattern was consistent across all load levels.

Such irregular variations indicate that wear behavior in wood is governed by complex tribological phenomena, involving mechanism transitions as sliding speed changes. At low speeds, prolonged contact can favor adhesive and microcutting wear, which increase surface degradation. At intermediate speeds, the formation of a tribofilm or selfpolishing effect can reduce wear. Similar behaviors were observed in aluminum alloys where tribo-films formed adaptively under variable surface interactions, reducing wear during sliding (Silva et al., 2023). However, at higher speeds, the increased frictional heating and surface fatigue lead to accelerated fiber damage in wood, mirroring transitions from mild to severe wear seen in ductile alloys with increasing speed.

A broader perspective on non-monotonic behavior is provided by Brink et al. (2020), who developed a parameter-free model for adhesive wear, showing that particle detachment rates vary nonlinearly with sliding conditions due to evolving contact mechanics and detachment thresholds. These findings support the idea that speed not only changes the energy input and temperature at the interface but also triggers shifts in the dominant wear mechanisms, debris removal efficiency, and tribofilm formation all crucial factors in wood tribology. Finally, analogous behavior has been observed by Zhang et al. (2022) in degradation of polymer composites under sliding: an optimal speed window minimizes wear, while both lower and higher speeds lead to increased wear due to shifts between abrasive and fatigue mechanisms

This implies that there exists an optimal speed range for each wood species, at which the wear coefficient reaches a minimum. Identifying these thresholds can inform the design of wood components exposed to frictional loading in order to maximize wear resistance under practical use conditions.

3.5 COMPARATIVE ANALYSIS OF THE EFFECT OF SPEED ON WEAR BEHAVIOR ACROSS SPECIES

The influence of sliding speed on the wear behavior of *Thieghemella heckelii* (makore), *Khaya anthotheca* (mahogany), and *Pericopsis elata* (assamela) was examined under three load levels: 250 g, 500 g, and 750 g. The results, presented in Table 2, show that the wear coefficient does not evolve linearly with speed but instead reveals species specific critical ranges where wear is either minimized or exacerbated.

Table 2
Speeds valus for minimal, mean and maximal wear for Makore, Mahogany and Assamela tested at different values of loads

Wear coefficient				
Species	Loads	Minimal	mean	Maximal
Makore	250g	40rpm	60rpm	20rpm
	500g	30rpm	40rpm	50rpm
	750g	70rpm	30 et 50rpm	20rpm
Mahogany	250g	50rpm	20 et 40rpm	30rpm
	500g	40rpm	20 et 60rpm	30rpm
	750g	30rpm	40rpm	20rpm
Assamela	250g	30 et 60rpm	20 et 60rpm	70rpm
	500g	60rpm	30rpm	70rpm
	750g	50rpm	60rpm	30rpm

3.5.1 *Makore (Thieghemella heckelii)*

Makore shows a relatively predictable pattern, especially under increasing loads:

- At 250 g, the lowest wear coefficient is observed at 40 rpm, while the maximum is found at 20 rpm, highlighting that low speeds are unfavorable.

- At 500 g, wear is minimized at 30 rpm, with a progressive increase up to a peak at 50 rpm.
- At 750 g, *makoré* presents an interesting case where 70 rpm gives the lowest wear, while 20 rpm again causes the highest. Mean wear values at 30 and 50 rpm suggest a broader plateau of acceptable performance.

These trends imply that *makoré*, owing to its fine grain and high density, is more resilient at high speeds, especially under heavier loads possibly due to improved fiber compaction and load distribution across its cellular matrix.

3.5.2 *Mahogany (Khaya anthotheca)*

In contrast, *mahogany* displays more irregular and load-sensitive behavior:

- At 250 g, 50 rpm results in the lowest wear coefficient, while the maximum occurs at 30 rpm. The mean falls between 20 and 40 rpm.
- At 500 g, 40 rpm yields the lowest wear, with 30 rpm again causing peak values indicating that this speed level may mark a transition to a more damaging wear mechanism.
- At 750 g, wear is lowest at 30 rpm and highest at 20 rpm, suggesting a strong vulnerability to slow-speed adhesive wear.

These results may stem from *mahogany's* relatively porous structure and large vessel elements, which likely promote localized failure, cell wall buckling, and insufficient energy dissipation during prolonged contact at low speeds.

3.5.3 *Assamela (Pericopsis elata)*

Assamela shows variable behavior but appears less sensitive to moderate speeds:

- At 250 g, 30 and 60 rpm give the lowest wear, while 70 rpm leads to peak wear possibly due to thermal degradation at high friction speeds.
- At 500 g, 60 rpm remains optimal, with wear increasing significantly at 70 rpm.
- At 750 g, the optimal speed is 50 rpm, while the maximum wear again shifts to 30 rpm, indicating possible early fatigue failure.

These findings suggest that *assamela*, though dense and fibrous, may suffer from a threshold effect where high speeds induce heat-related wear, while low speeds promote mechanical fatigue. The intermediate range (50–60 rpm) appears most stable for this species.

A key observation across all species is that 20 rpm frequently correlates with the highest wear coefficient, especially for *makoré* and *mahogany*. This confirms that very low sliding speeds are unfavorable, possibly due to:

- Increased surface adhesion time,
- Accumulation of debris at the interface,
- Lack of sufficient kinetic energy to initiate fiber fracture cleanly.

Conversely, the 30–50 rpm range emerges as the most wear-efficient zone for all species, particularly under moderate and high loads. These results underline the necessity of species-specific wear optimization, as the microstructural characteristics deeply affect how a given wood responds to tribological stress. From a design perspective, selecting operating speed ranges that avoid extremes can significantly extend the service life of wood components in wear-prone applications.

4. CONCLUSION

This study highlights the complex tribological behavior of three tropical wood species *Thieghemella heckelii* (makoré), *Khaya anthotheca* (mahogany), and *Pericopsis elata* (assamela) under dry two-body abrasive conditions, with sliding applied perpendicular to the grain. The analysis based on wear volume versus sliding distance confirms that, for all test conditions, the materials exhibit a linear relationship in the steady-state wear region. This trend aligns with Archard's wear law and validates the use of the wear coefficient (k) as a representative indicator of long-term material degradation.

Unexpectedly, the wear coefficient was found to decrease as load increased across all sliding speeds. A pronounced negative slope was observed between 250 g and 500 g, followed by a more moderate decline from 500 g to 750 g. This behavior, which contrasts with classical wear theory, suggests that higher loads may promote improved fiber compaction and stress homogenization, limiting surface fragmentation and reducing interfacial damage in these hardwoods.

The effect of sliding speed revealed non-linear and species-dependent trends. Makore showed superior performance at higher speeds and heavier loads, while wear increased significantly at low speeds. Mahogany responded best under dual conditions: high-speed/low-load and low-speed/high-load, indicating sensitivity to load-speed synergy. Assamela demonstrated the most stable behavior overall, with minimal wear around intermediate speeds (50–60 rpm) and increased degradation at very low or very high speeds due to fatigue and thermal effects, respectively.

Altogether, these findings emphasize the need for species-specific wear optimization strategies, particularly in engineering applications where tropical hardwoods are exposed to repeated contact or motion. The observed behaviors reinforce that wear is governed not only by external parameters such as load and speed, but also by internal anatomical features including fiber orientation, porosity, vessel size, and structural density which control how each species dissipates mechanical stress during frictional interactions.

Future work could incorporate 3D profilometry or microscopic surface analysis to further understand the dominant wear mechanisms involved, particularly at extreme operating conditions.

Références:

1-**Wu, G., Yan, Q., Zhou, Y., Wang, B., Luo, Z., Ma, C., & Yu, B. (2025**). *Friction and Wear Properties of Densified Wood*. Tribology, 45(9), 1–13. https://doi.org/10.16078/j.tribology.2024170

2-**Snow, D., Khademibami, L., Sherrington, A., Shmulsky, R., Montague, I., Ross, R. J., & Wang, X. (2022).** *Effect of Thermomechanical Densification Treatment on Abrasion Resistance of Five US Hardwoods*. Forest Products Journal, 72(3), 175–179. https://doi.org/10.13073/FPJ-D-22-00028

3-**Nasir, V., & Cool, J. (2018).** *A review on wood machining: characterization, optimization, and monitoring of the sawing process*. Wood Material Science & Engineering, 15(3), 1–16. https://doi.org/10.1080/17480272.2018.1465465

4-Torkghashghaei, M., Shaffer, W., Ugulino, B., Georges, R., Hernández, R. E., & Blais, C. (2022). *Improvement of the Wear Resistance of Circular Saws Used in the First Transformation of Wood through the Utilization of Variable Engineered MicroGeometry Performed on PVDCoated WCCo Tips*. Applied Sciences, 12(23), 12213. https://doi.org/10.3390/app122312213

5-Gendvilas, V., Downes, G. M., Lausberg, M., Harrington, J. J., & Lee, D. J. (2024). *Predicting Wood Density Using Resistance Drilling: The Effect of Varying Feed Speed and RPM*. Forests, 15(4), 579. https://doi.org/10.3390/f15040579

6-Ghadiri, M., Azdast, T., & Heravi, G. (2021). *Effect of tool wear and cutting parameters on wear mechanisms in machining laminated wood composites*. Wear, 476, 203521. https://doi.org/10.1016/j.wear.2020.203521

7-**Tenorio, C., & Moya, R. (2020).** *Effect of thermohydromechanical densification on the wood properties of three shortrotation forest species in Costa Rica.* BioResources, 15(4), 8065–8084. https://doi.org/10.15376/biores.15.4.8065-8084

8-**Zhou, Q., Chen, C., Tu, D., Zhu, Z., & Li, K. (2019).** *Surface densification of poplar solid wood: Effects of the process parameters on the density profile and hardness.* BioResources, 14(2), 4814–4831. https://doi.org/10.15376/biores.14.2.4814-4831

9- **Leiter, L. M., Myna, R., Frömel-Frybort, S., et al. (2022).** *Triboelectric surface field strength of wood after brushing.* Wood Science and Technology, 56(6), 1401–1417. https://doi.org/10.1007/s00226-022-01411-z

10-**Okokpujie, I. P., Tartibu, L. K., Musa-Basheer, H. O., & Adeoye, A. O. M. (2024).** Effect of coatings on mechanical, corrosion and tribological properties of industrial materials: a comprehensive review. *Journal of Bio-and Tribo-Corrosion*, *10*(1), 2. https://doi.org/10.1007/s40735-023-00805-1

11-**Sakhamuri, M. S. D., Harvey, T. J., Vierneusel, B., & Wood, R. J. (2023).** Wear induced changes in surface topography during running-in of rolling-sliding contacts. *Wear*, *522*, 204685. https://doi.org/10.1016/j.wear.2023.204685

12-**Zambrano, O. A., Iglesias-Guerrero, B., Rodríguez, S. A., & Coronado, J. J. (2024).** Running-in period during sliding wear of austenitic steels. *Tribology Letters*, *72*(3), 70. https://doi.org/10.1007/s11249-024-01867-z

13-**Abdelbary, A. (2021).** Friction and wear of polymer and polymer composites. In *Tribology of Polymer and Polymer Composites for Industry 4.0* (pp. 33–54). Singapore: Springer Singapore. https://doi.org/10.1007/978-981-16-3903-6_3

14-**Zhai, W., Bai, L., Zhou, R., Fan, X., Kang, G., Liu, Y., & Zhou, K. (2021).** Recent progress on wear-resistant materials: designs, properties, and applications. *Advanced Science*, *8*(11), 2003739. https://doi.org/10.1002/advs.202003739

15-**Silva, R. D., Martins, P. A., & Santos, M. (2023).** *Tribofilm formation and wear reduction in dry sliding of aluminum alloys*. Advanced Engineering Materials, 180, e14002. https://doi.org/10.1002/adem.202400142

16-**Brink, T., Frérot, L., & Molinari, J.-F. (2020).** *A parameter-free mechanistic model of the adhesive wear process of rough surfaces in sliding contact*. Journal of the Mechanics and Physics of Solids, 145, 104238. https://doi.org/10.1016/j.jmps.2020.104238

17-**Zhang, X., Liu, Y., Wang, J., & Huang, R. (2022).** *Non-monotonic wear response in polymer composites under varying sliding speeds: optimal speed regimes and mechanism transitions*. Materials, 17(2), 281. https://doi.org/10.3390/ma17020281

References

1. **Wu, G., Yan, Q., Zhou, Y., Wang, B., Luo, Z., Ma, C., & Yu, B. (2025**). *Friction and Wear Properties of Densified Wood*. Tribology, 45(9), 1–13. https://doi.org/10.16078/j.tribology.2024170
2. **Snow, D., Khademibami, L., Sherrington, A., Shmulsky, R., Montague, I., Ross, R. J., & Wang, X. (2022).** *Effect of Thermomechanical Densification Treatment on Abrasion Resistance of Five US Hardwoods*. Forest Products Journal, 72(3), 175–179. https://doi.org/10.13073/FPJ-D-22-00028
3. **Nasir, V., & Cool, J. (2018).** *A review on wood machining: characterization, optimization, and monitoring of the sawing process*. Wood Material Science & Engineering, 15(3), 1–16. https://doi.org/10.1080/17480272.2018.1465465
4. **4-Torkghashghaei, M., Shaffer, W., Ugulino, B., Georges, R., Hernández, R. E., & Blais, C.** (2022). *Improvement of the Wear Resistance of Circular Saws Used in the First Transformation of Wood through the Utilization of Variable Engineered Micro-Geometry Performed on PVD-Coated WC-Co Tips*. Applied Sciences, 12(23), 12213. https://doi.org/10.3390/app122312213
5. **5-Gendvilas, V., Downes, G. M., Lausberg, M., Harrington, J. J., & Lee, D. J.** (2024). *Predicting Wood Density Using Resistance Drilling: The Effect of Varying Feed Speed and RPM*. Forests, 15(4), 579. https://doi.org/10.3390/f15040579
6. **6-Ghadiri, M., Azdast, T., & Heravi, G.** (2021). *Effect of tool wear and cutting parameters on wear mechanisms in machining laminated wood composites*. Wear, 476, 203521. https://doi.org/10.1016/j.wear.2020.203521
7. 7-**Tenorio, C., & Moya, R. (2020).** *Effect of thermo-hydro-mechanical densification on the wood properties of three short-rotation forest species in Costa Rica.* BioResources, 15(4), 8065–8084. https://doi.org/10.15376/biores.15.4.8065-8084
8. **Zhou, Q., Chen, C., Tu, D., Zhu, Z., & Li, K. (2019).** *Surface densification of poplar solid wood: Effects of the process parameters on the density profile and hardness.* BioResources, 14(2), 4814–4831. https://doi.org/10.15376/biores.14.2.4814-4831
9. **Leiter, L. M., Myna, R., Frömel-Frybort, S., et al. (2022).** *Triboelectric surface field strength of wood after brushing.* Wood Science and Technology, 56(6), 1401–1417. https://doi.org/10.1007/s00226-022-01411-z
10. **Okokpujie, I. P., Tartibu, L. K., Musa-Basheer, H. O., & Adeoye, A. O. M. (2024).** Effect of coatings on mechanical, corrosion and tribological properties of industrial materials: a comprehensive review. *Journal of Bio-and Tribo-Corrosion*, *10*(1), 2. https://doi.org/10.1007/s40735-023-00805-1

11. **Sakhamuri, M. S. D., Harvey, T. J., Vierneusel, B., & Wood, R. J. (2023).** Wear induced changes in surface topography during running-in of rolling-sliding contacts. *Wear*, *522*, 204685. https://doi.org/10.1016/j.wear.2023.204685
12. **Zambrano, O. A., Iglesias-Guerrero, B., Rodríguez, S. A., & Coronado, J. J. (2024).** Running-in period during sliding wear of austenitic steels. *Tribology Letters*, *72*(3), 70. https://doi.org/10.1007/s11249-024-01867-z
13. **Abdelbary, A. (2021).** Friction and wear of polymer and polymer composites. In *Tribology of Polymer and Polymer Composites for Industry 4.0* (pp. 33-54). Singapore: Springer Singapore. https://doi.org/10.1007/978-981-16-3903-6_3
14. **Zhai, W., Bai, L., Zhou, R., Fan, X., Kang, G., Liu, Y., & Zhou, K. (2021).** Recent progress on wear-resistant materials: designs, properties, and applications. *Advanced Science*, *8*(11), 2003739. **https://doi.org/10.1002/advs.202003739**
15. **Silva, R. D., Martins, P. A., & Santos, M. (2023).** *Tribofilm formation and wear reduction in dry sliding of aluminum alloys*. Advanced Engineering Materials, 180, e14002. https://doi.org/10.1002/adem.202400142
16. **Brink, T., Frérot, L., & Molinari, J.-F. (2020).** *A parameter-free mechanistic model of the adhesive wear process of rough surfaces in sliding contact*. Journal of the Mechanics and Physics of Solids, 145, 104238. https://doi.org/10.1016/j.jmps.2020.104238
17. **Zhang, X., Liu, Y., Wang, J., & Huang, R. (2022).** *Non-monotonic wear response in polymer composites under varying sliding speeds: optimal speed regimes and mechanism transitions*. Materials, 17(2), 281. https://doi.org/10.3390/ma17020281

Figures

Figure 1

(a) Wear test device, (b) balance, and (c) worn and unworn specimens

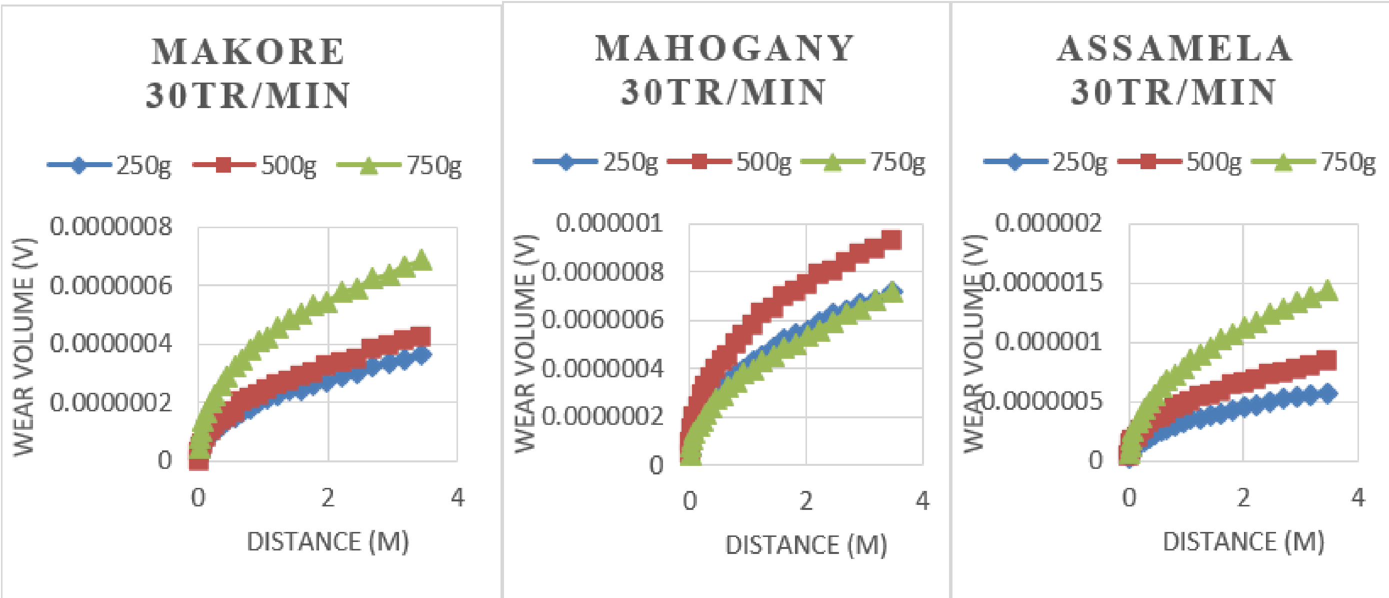

Figure 2

Variation of wear volume as a function of rolling distance for Makore (Tieghemella heckelii), Mahogany (Khaya anthotheca), and Assamela (Pericopsis elata) at a constant rotational speed of 30 rpm, under three normal loads (250 g, 500 g, and 750 g).

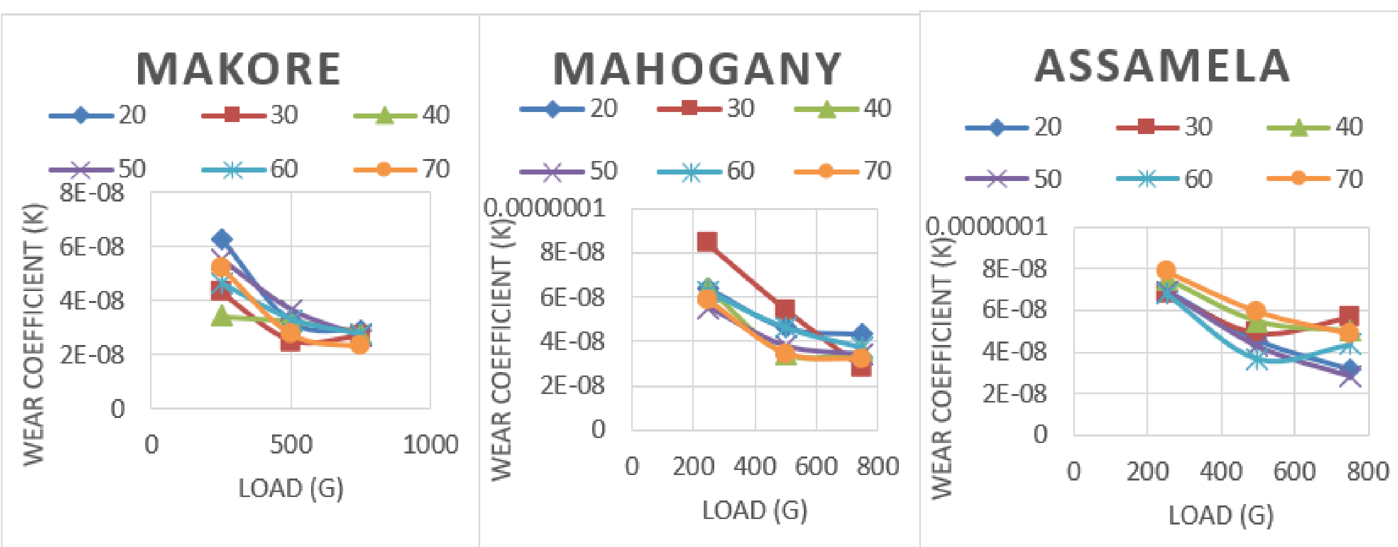

Figure 3

Evolution of the wear coefficient as a function of applied load for Makore (Tieghemella heckelii), Mahogany (Khaya anthotheca), and Assamela (Pericopsis elata), evaluated across multiple rotational speeds (20–70 rpm)

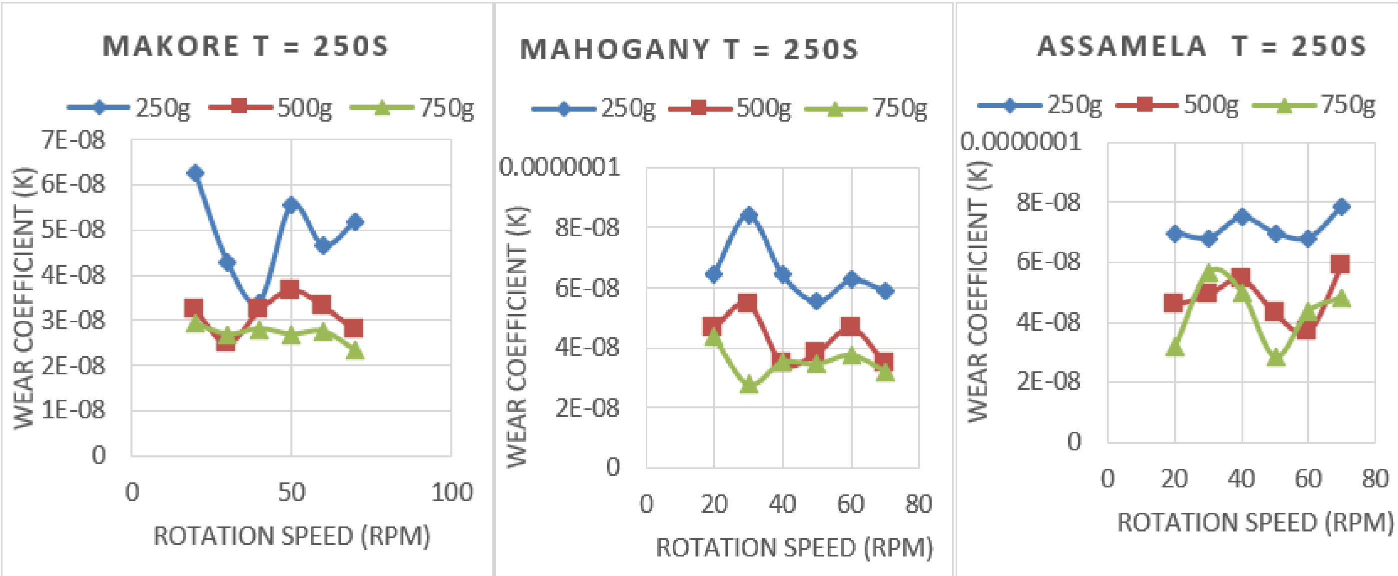

Figure 4

Variation of the wear coefficient as a function of sliding speed for Makore (Tieghemella heckelii), Mahogany (Khaya anthotheca), and Assamela (Pericopsis elata) at different applied load levels (250 g, 500 g, and 750 g).

Supplementary Files

This is a list of supplementary files associated with this preprint. Click to download.

- makor.xlsx